Science of the Total Environment 945 (2024) 173864

Contents lists available at ScienceDirect

Science of the Total Environment

journal homepage: www.elsevier.com/locate/scitotenv

Microplastics enhanced the allelopathy of pyrogallol on toxic *Microcystis* with additional risks: Microcystins release and greenhouse gases emissions

Linqing Du [a], Qinglong Liu [a], Lan Wang [a], Honghong Lyu [b], Jingchun Tang [a,*]

[a] Key Laboratory of Pollution Processes and Environmental Criteria (Ministry of Education)/Tianjin Engineering Center of Environmental Diagnosis and Contamination Remediation, College of Environmental Science and Engineering, Nankai University, Tianjin 300350, China
[b] Tianjin Key Laboratory of Clean Energy and Pollution Control, School of Energy and Environmental Engineering, Hebei University of Technology, Tianjin 300401, China

HIGHLIGHTS

- Microplastics exhibited a synergistic effect with higher concentration of pyrogallol on allelopathy.
- In high PYR treatments, PS notably boosted both intracellular and extracellular MCs levels.
- Greenhouse gas emission was enhanced by PS in high PYR treatment
- Microplastics present ecological risks by enhancing allelopathy effect.

GRAPHICAL ABSTRACT

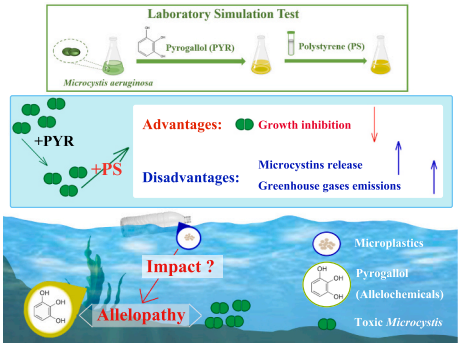

ARTICLE INFO

Editor: Susanne Brander

Keywords:
Microplastics
Allelopathy
Synergistic effect
Microcystins
Greenhouse gases

ABSTRACT

Cyanobacteria blooms (CBs) caused by eutrophication pose a global concern, especially *Microcystis aeruginosa* (*M. aeruginosa*), which could release harmful microcystins (MCs). The impact of microplastics (MPs) on allelopathy in freshwater environments is not well understood. This study examined the joint effect of adding polystyrene (PS-MPs) as representative MPs and two concentrations (2 and 8 mg/L) of pyrogallol (PYR) on the allelopathy of *M. aeruginosa*. The results showed that the addition of PS-MPs intensified the inhibitory effect of 8 mg/L PYR on the growth and photosynthesis of *M. aeruginosa*. After a 7-day incubation period, the cell density decreased to 69.7 %, and the chl-*a* content decreased to 48 % compared to the condition without PS-MPs ($p < 0.05$). Although the growth and photosynthesis of toxic *Microcystis* decreased with the addition of PS-MPs, the addition of PS-MPs significantly resulted in a 3.49-fold increase in intracellular MCs and a 1.10-fold increase in extracellular MCs ($p < 0.05$). Additionally, the emission rates of greenhouse gases (GHGs) (carbon dioxide, nitrous oxide and methane) increased by 2.66, 2.23 and 2.17-fold, respectively ($p < 0.05$). In addition, transcriptomic analysis showed that the addition of PS-MPs led to the dysregulation of gene expression related to DNA synthesis, membrane function, enzyme activity, stimulus detection, MCs release and GHGs emissions in *M. aeruginosa*. PYR and PS-MPs triggered ROS-induced membrane damage and disrupted photosynthesis in algae, leading to increased MCs and GHG emissions. PS-MPs accumulation exacerbated this issue by impeding light

* Corresponding author at: College of Environmental Science and Engineering, Nankai University, 38 Tongyan Road, Jinnan District, Tianjin 300350, China.
E-mail address: tangjch@nankai.edu.cn (J. Tang).

https://doi.org/10.1016/j.scitotenv.2024.173864
Received 21 January 2024; Received in revised form 16 May 2024; Accepted 7 June 2024
Available online 13 June 2024

absorption and membrane function, further heightening the release of MCs and GHGs emissions. Therefore, PS-MPs exhibited a synergistic effect with PYR in inhibiting the growth and photosynthesis of *M. aeruginosa*, resulting in additional risks such as MCs release and GHGs emissions. These results provide valuable insights for the ecological risk assessment and control of algae bloom in freshwater ecosystems.

1. Introduction

Cyanobacterial blooms (CBs) are a pressing global concern linked to accelerated eutrophication in aquatic ecosystems (Wang et al., 2023b). These blooms pose significant threats, poisoning fish and other aquatic fauna, disrupting ecosystem integrity, and endangering human health (Plaas and Paerl, 2021). *Microcystis aeruginosa* (*M. aeruginosa*), a prevalent cyanobacteria genus, stands out as the primary organism responsible for harmful algal blooms, mainly due to its release of microcystins (MCs) (Miles et al., 2012). The allelopathy between plants and cyanobacteria has gained attention as a cost-effective and eco-friendly biological control for CBs (Zhu et al., 2021). Allelopathy involves the direct or indirect harmful effects of plants (including microorganisms) on other organisms through the production and release of allelochemicals into the environment (Zhu et al., 2021). Pyrogallol (PYR), among these allelochemicals, has raised concerns due to its significant growth inhibition on *M. aeruginosa* (Gao et al., 2020). Nakai et al. (2000) suggested that the macrophyte *Myriophyllum spicatum* released pyrogallol as allelochemical. Previous studies have indicated that pyrogallol affected algal growth; for instance, Shan et al. (2011) used chl-*a* content in algal cells as a growth indicator to investigate the impact of pyrogallol at different concentrations (0.5, 1, 2, 4 mg/L) on the growth of *Chlorella pyrenoidosa Chick*. Their results revealed that 4 mg/L of pyrogallol had the strongest inhibitory effect on *Chlorella pyrenoidosa Chick*. Wang et al. (2016a) found that a substantial suppression of both growth and pigment levels in *M. aeruginosa* TY001 upon exposure to pyrogallol. The inhibition mechanism of pyrogallol on *Microcystis* may involve interactions between proteins (Spencer et al., 1988), inhibition of alkaline phosphatase (Dziga et al., 2007), disruption of the electron transport chain, and oxidative damage due to polyphenol autoxidation (Nakai et al., 2001; Shao et al., 2009).

Human activities have led to a substantial increase in plastics production (Barnes, 2019), resulting in the release of microplastics (MPs) (Laskar and Kumar, 2019; Sobhani et al., 2020). MPs, due to their small size and toxic potential, have received concerns about their adverse effects on aquatic ecosystems (Amaneesh et al., 2023). Wu et al. (2021) concluded that smaller-sized polystyrene (PS) did not necessarily imply increased toxicity; in fact, 1 μm PS had a greater adverse effect on *M. aeruginosa* than 100 nm PS. In other cases, MPs were shown to have a detrimental impact on algae, chiefly through mechanisms of adsorption and shading (Wang et al., 2023c). Nevertheless, some research indicated that PS could enhance algal growth. Mao et al. (2018) observed that from the end of the logarithmic stage to the fixed stage, the adverse effects of PS were reduced by cell wall thickening, algae homopolymers and algae-MPs heterogeneous aggregation, which led to the increase of photosynthetic activity and growth of algae, and the cell structure returned to normal. The utilization of MPs also had an impact on greenhouse gases (GHGs) emissions. During MPs exposure, the release of organic matter could affect the carbon and nitrogen cycles of the ecosystems, indicating that MPs could modulate GHGs emissions (Sun et al., 2020; Zhang et al., 2022).

Moreover, the combined toxicity of MPs with other pollutants has also attracted attention, with studies showing antagonistic or synergistic effects on toxicity to various organisms (Shi et al., 2021; Liu et al., 2022a; Zhang et al., 2024). For example, PS was found to mitigate the adverse effects of excess boron on *M. aeruginosa*; however, PS-NH_2, after modification with cationic amino groups ($-NH_2$), intensified the inhibitory effect of excessive boron on *M. aeruginosa*. This was attributed to the charge alteration on PS, which affected its adsorption of boron and the aggregation behavior between MPs and algal cells (Zhang et al., 2023). Moreover, research demonstrated that combined exposure to PS and nonylphenol (NP) alleviated the toxicity of NP to algae compared to NP treatment alone; after 96 h, algae co-treated with PS and NP exhibited elevated cell densities, increased pigment concentrations, reduced levels of extracellular proteins, and better preservation of intracellular structural integrity (Jin et al., 2022). On another note, numerous researchers have also uncovered that MPs amplified the toxicity of coexisting pollutants to aquatic organisms. Specifically, the synergistic effect of MPs and malathion has been shown to enhance the bioaccumulation capacity of *Minuca ecuadoriensis* while concurrently reducing survival rates (Villegas et al., 2022). The presence of MPs intensified the toxicity of copper to zebrafish livers and intestines, potentially through inhibited copper-ion transport and exacerbating oxidative stress, thereby heightened the toxic impact of copper (Qiao et al., 2019). MPs augmented the toxicity of pollutants to aquatic life, manifested in elevated cellular toxicity, endocrine disruption, immunotoxicity, and a significant increase in oxidative stress (Sun et al., 2022). However, these studies focused on the relationship between MPs and pollutants, overlooking the interference behavior of MPs on the substances produced in the aqueous system with special functions in the water ecosystem such as PYR. To address this gap, we investigated the impact of MPs on the allelopathy effect between PYR and *M. aeruginosa*.

In this study, PYR was used as allelochemicals, polystyrene (PS-MPs) as MPs, and *M. aeruginosa*, known for MCs release as the target cyanobacteria. We comprehensively examined the effects of PS-MPs on the allelopathy effect between PYR and *M. aeruginosa* by assessing changes in physiological parameters, antioxidant enzymes, MCs release, and GHGs emission rates of *M. aeruginosa*. Our study hypothesized that the addition of MPs would enhance the allelopathy of PYR on toxic *Microcystis*, since the combined presence of MPs and PYR was believed to impair algal photosynthesis through light obstruction and induce excessive reactive oxygen species (ROS) production in algal cells, which in turn attacked and damaged the algae. These findings will provide valuable insights into the ecological risks posed by MPs, contributing to a better understanding of the emerging crises in aquatic ecosystems.

2. Materials and methods

2.1. Algal cultivation

M. aeruginosa (FACHB-942) were purchased from Freshwater Algae Culture Collection of the Institute of Hydrobiology, Wuhan, Hubei Province, China. The algal cells were cultivated in 250 mL conical flasks containing 150 mL of the sterilized BG-11 medium at 25 ± 1 °C under a photoperiod of 12 L:12D (light intensity: 4000 lx).

2.2. Chemicals

PS-MPs microspheres aqueous suspension (25 g/L) with diameter of 1 μm (Wu et al., 2021; Zhou et al., 2021) was purchased from Tianjin BaseLine and dispersed totally by sonication before use. The properties of PS-MPs were provided in Fig. S1. PYR from Heowns was dissolved in Milli-Q water before use.

2.3. Experimental design

The PS-MPs solution was added into the algal medium to obtain the final concentrations of 25 mg/L based on previous studies (Jambeck

et al., 2015; Chen et al., 2020; Li et al., 2020a). We selected lower and higher concentrations of 2 mg/L and 8 mg/L of PYR, respectively, in our experiment, both of which were found to have allelopathy effect on *M. aeruginosa*, guided by the previous researches (Liu et al., 2007; Wang et al., 2016a). Then PS-MPs and PYR were added alone (The PYR concentrations at 2 mg/L and 8 mg/L were denoted as "PYR_2" and "PYR_8" respectively.) or together (expressed as "PYR_2 + PS" and "PYR_8 + PS" respectively) to the algal medium. Algal cultures with no PS-MPs and PYR were used as a control (CK). The algal cells in the exponential phase were prepared for the experiments at an initial density of 10^6 cells/mL. All flasks were shaken manually 3 times daily and incubated for 7 days under the culture conditions described above. Three replicates were used for all treatments and analyses.

2.4. Physiology measurements

Cell density was calculated with an optical microscope (Olympus CX31) every second day. Chlorophyll *a* (chl-*a*) is a widely used indicator of algal growth (Wei et al., 2010). After exposure for 7 days, 10 mL samples of *M. aeruginosa* from different treatments were subjected to centrifugation at 4000 rpm for 5 min at 4 °C. The precipitates were extracted using 95 % ethanol in the dark overnight at 4 °C. The extracts were then centrifuged at 8000 rpm for 10 min at 4 °C, and the supernatants were analyzed using an ultraviolet spectrophotometer (T6 New Century, Beijing Persee General Instrument Co., Ltd., China) at 665 and 649 nm. The content of chl-*a* was calculated by the following equation (Wang et al., 2013):

$$\text{Chlorophyll } a = 13.7 \times OD_{665} - 5.76 \times OD_{649}$$

The alterations in chlorophyll fluorescence parameters also pointed to the damage caused by contaminants on the algal cells photosynthetic capacity (Wang et al., 2019). The photosynthetic parameters of the algal cells, including photosynthetic efficiency (Fv/Fm), quantum yield of PSII (Y(II)) and electron transport rate (ETR) were investigated using a pulse-amplitude-modulation fluorimeter (WATERPAM, Heinz Walz, Effeltrich, Germany) following a 6-minute dark adaptation period for the algal cells (Hou et al., 2023).

2.5. Cell morphology

The morphological changes of algal cells were studied using a Scanning Electron Microscope (SEM) (FE-SEM, JEOL, JSM-7800F). After 7 days of exposure under individual and combined tests, 10 mL samples of the algal cells were collected through centrifugation (8000 rpm, 10 min). The algal cells were initially fixed with 2.5 % glutaraldehyde for 4 h. Subsequently, they underwent a series of dehydration steps using alcohol solutions of 30 %, 50 %, 70 %, 80 % and 90 % for 15 min each, followed by two rounds of 100 % alcohol for 20 min each. After fixation with tert-butyl alcohol, the samples were freeze-dried. Finally, the lyophilized powders were mounted on a conductive adhesive, gold-coated, and prepared for final observation (Wang et al., 2021a).

2.6. Antioxidant measurements

For enzyme activity measurement, 10 mL samples of the algal cells exposed to individual and combined tests for 7 days were collected. The collections were centrifuged at 8000 rpm for 10 min at 4 °C. Subsequently, the cells were resuspended in a phosphate buffer solution (PBS, pH 7.2–7.4). To disrupt the cells and extract the enzyme contents, the suspension underwent ultrasonication on an ice bath (200 W, 3 s at 10 s intervals). The superoxide dismutase (SOD) (Solarbio, Beijing, China), lactate dehydrogenase (LDH) (Solarbio, Beijing, China) and malondialdehyde (MDA) (Nanjing Jiancheng Bioengineering Institute, China) were measured using the respective assay kits. All measurements were performed following the manufacturer's instructions (Liu et al., 2023).

2.7. ROS determination

Reactive oxygen species (ROS) level was assessed using a ROS detection kit (Beyotime Institute of Biotechnology). After 7 days of exposure, the cells were harvested through centrifugation and then suspended in a final concentration of 10 μmol/L of 2′,7′-dichlorodihydrofluorescein diacetate (DCFH-DA). Subsequently, the algal cells were incubated in an incubator at 37 °C for 20 min. Afterward, they underwent three washes with PBS. Finally, the cells were resuspended in PBS and subjected to measurement using a microplate reader (Synergy H4, Bio-Tek, Vermont, USA) with an excitation wavelength of 488 nm and an emission wavelength of 525 nm (Liu et al., 2022b).

2.8. MCs determination

After 7 days of incubation, the algal cells were collected and centrifuged at 8000 rpm for 10 min at 4 °C. The supernatant, containing extracellular MCs (extra-MCs), was filtered through a 13 mm diameternylon syringe filter (0.22 μm pore size) for analysis (Zheng et al., 2021b). The sediment was resuspended in PBS and ultrasonicated on an ice bath (200 W, 3 s at 10 s intervals). After centrifugation, the obtained supernatant was tested for intracellular MCs (intra-MCs). Both intra-MCs and extra-MCs were measured using the MCs ELISA kit (Jiangsu Meimian Industrial, Yancheng, Jiangsu, China) (Zhang et al., 2023).

2.9. GHGs detection

The GHGs flux of *M. aeruginosa* was measured by G2508 Green Gas analyzer (Picarro Inc., Santa Clara, CA, USA). The GHGs collection device diagram was shown in Fig. S2. To investigate the variation in GHGs emission rates over time, observations were made every two days. Briefly, the algal cells were enclosed in a static closed chamber connected to the analyzer for approximately 20 min. Within this period, the concentrations of carbon dioxide (CO_2), nitrous oxide (N_2O) and methane (CH_4) were measured and the gas emission rates were then calculated using the following equation (Zhen et al., 2018; Ren et al., 2020; Liu et al., 2021; Zhang et al., 2022):

$$F = \frac{(C_f - C_i) \times V}{\Delta t \times n} \times \frac{P}{P_0} \times \frac{T_0}{T} \times k$$

Among them:

F [μg/(10^6 cells)/h] corresponds to the release rates of different GHGs, the unit represents the amount of GHGs emitted per million cells per hour;

V (1.25×10^{-3} m^3) denotes the total volume of GHGs, encompassing both pipelines and gas chambers;

C_i and C_f (μL/L) depict the initial and concluding GHGs concentrations;

T (K) and P (kPa) correspond to the absolute temperature and absolute pressure during the GHGs measurement process;

T_0 (273.15 K) and P_0 (101.325 kPa) indicate the absolute temperature and absolute pressure under standard conditions;

Δt (h) signifies the duration for GHGs measurement;

n (10^6 cells) denotes the quantity of the algal cells in the culture flask;

k (μg/m^3) represents the correlation coefficient used to convert ppm into mass concentration (μg/m^3) under ideal conditions. The conversion coefficients for CO_2, N_2O and CH_4 are 1.96×10^3, 1.96×10^3 and 0.71×10^3, respectively.

2.10. Transcriptomic analysis

After 7 days exposure to 25 mg/L of PS-MPs and 8 mg/L of PYR, total RNA was extracted from *M. aeruginosa* cultures using TRIzol® Reagent. Subsequently, we prepared the RNA-seq transcriptome library using the

TruSeqTM RNA sample preparation Kit by Illumina (San Diego, CA), utilizing 2 μg of total RNA. The resulting data, generated via the Illumina platform, underwent bioinformatics analysis. All analyses were conducted through the freely accessible Majorbio Cloud Platform (www.majorbio.com) provided by Shanghai Majorbio Bio-pharm Technology Co., Ltd. To further elucidate the differentially expressed genes (DEGs), we subjected them to Gene ontology (GO) enrichment analysis and functional annotation. The detailed analysis processes and parameters settings were shown in Text 1.

2.11. Statistical analyses

The data were subjected to statistical analysis using GraphPad Prism Software Version 8.0 (San Diego, CA, USA), and the results were expressed as the mean ± standard deviation (SD). Statistical significance was determined using a one-way analysis of variance (ANOVA), followed by post-hoc Tukey's Honestly Significant Difference (HSD) test.

3. Results and discussion

3.1. Allelopathy effect of PYR and PS-MPs on M. aeruginosa

As depicted in Fig. 1a-b, the addition of PS-MPs into the culture system resulted in a 1.36-fold increase in cell density compared to CK following a 7-day incubation period. However, the addition of 8 mg/L of PYR significantly reduced cell density to 44.96 % of the CK after 5 days of incubation, further declining to 33.16 % of CK after 7 days of incubation ($p < 0.05$). These findings clearly demonstrated the inhibitory effect of PYR on the growth of *M. aeruginosa*, indicating its role as an allelochemical. Joint exposure experiments revealed that the cell density of PYR_8 + PS reduced to 69.7 % of PYR_8 after a 7-day incubation, indicating that PS-MPs further intensified the growth inhibition of *M. aeruginosa* under PYR_8 conditions. Conversely, no growth inhibition effect was observed in the 2 mg/L PYR system. Moreover, the chl-*a* content of PYR_8 + PS is reduced to 48 % of PYR_8 when compared to PYR_8 ($p < 0.05$). In contrast, the chl-*a* content of PYR_2 + PS resulted in a slight decrease of 0.58 % compared to PYR_2, although the difference was not statistically significant. The chlorophyll fluorescence parameters (Fv/Fm, Y(II) and ETR) exhibited a similar trend to that of chl-*a*. Notably, in the high PYR concentration treatment group, PYR_8 + PS significantly reduced chlorophyll fluorescence parameters compared to PYR_8 (Fv/Fm: 6.52 %, Y(II): 4.36 % and ETR: 11.41 %). Wu et al. (2021) also found that treatment with 1 μm PS-MPs led to an increase in algal growth, which was suggested to be due to the leached additives from MPs and the MPs themselves might serve as a substrate for algal growth. It has also been suggested that algae might respond to the environmental stress by proliferating (Kaur et al., 2022). This could explain the increased algal cell density observed under PS-MPs alone treatment in our study. The augmented inhibitory effect on *M. aeruginosa* growth observed in the co-exposure experiments under PS-MPs + PYR_8 conditions may be attributed to that PS-MPs facilitated the entry of PYR into cells by damaging algal cell structures, thereby enhanced toxicity, as proposed by Yi et al. (2019). Our findings, particularly the alterations in chl-*a* content and fluorescence parameters under high PYR concentration treatments, indicated that the intrusion of PS-MPs exacerbated the disruption of photosynthesis in *M. aeruginosa* by PYR (Wang et al., 2019). The toxicity of PYR on the PSII of *M. aeruginosa* primarily was supposed to be caused by targeting the active reaction centers and the acceptor side of electron transport, which resulted in substantial suppression of photosynthesis and established a pivotal mechanism through which PYR impacted the growth and metabolism of *M. aeruginosa* (Wang et al., 2016a). Aggregated MPs blocked light from reaching the photosynthetic centers of algal cells (Bhattacharya et al., 2010), creating a shading effect that decreased the intensity of photosynthesis and electron transfer rates (Cao et al., 2022), ultimately affecting algal growth. Collectively, these findings suggested that PS-MPs and PYR likely cooperated in their detrimental influence on algal cell photosynthesis.

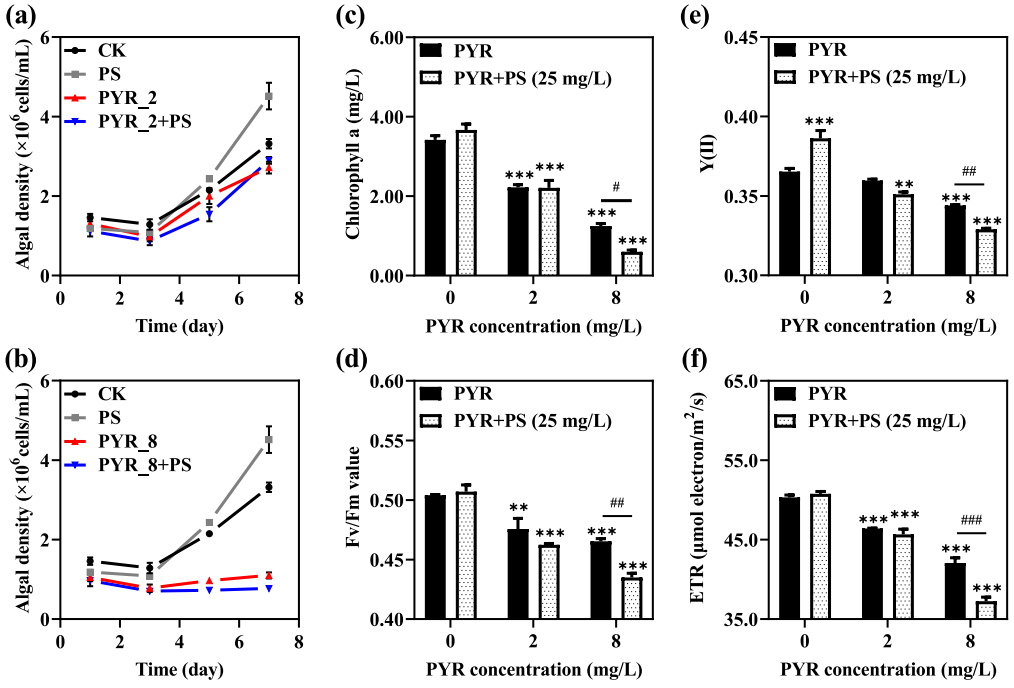

Fig. 1. Growth curve (a-b), chl-*a* (c), Fv/Fm (d), Y(II) (e) and ETR (f) of *M. aeruginosa* influenced by individual and combined exposure. Data were expressed as the mean ± SD. Significant differences between the control and treatments were indicated by asterisks (*), with the levels of significance denoted as $*p < 0.05$, $**p < 0.01$ and $***p < 0.001$. Horizontal lines with a pound (#) represented significant differences between the only PYR treatment and their combined treatments with PS-MPs, $\#p < 0.05$, $\#\#p < 0.01$, $\#\#\#p < 0.001$.

3.2. Oxidative damage of *M. aeruginosa*

Fig. 2a showed the morphology of *M. aeruginosa* in CK. Furthermore, Fig. 2b illustrated the adherence of PS-MPs to *M. aeruginosa* in PS-MPs treatment. As shown in the Fig. 2c-d, cell membrane damage in the algal cells were shown clearly in PYR and PYR + PS treatment. To explore the toxic mechanism of PS-MPs and PYR on *M. aeruginosa*, we further investigated ROS, SOD, MDA and LDH of *M. aeruginosa* under individual and combined treatments after 7 days (Fig. 2e-h). Fig. 2e illustrated that the ROS level of *M. aeruginosa* exposed to PYR_8 is 2.74-fold greater than that of CK, indicating oxidative stress by high PYR concentration. The addition of PS-MPs further significantly intensified ROS production by 1.72-fold ($p < 0.05$) compared to PYR_8. Fig. 2f showed the SOD values of *M. aeruginosa* under two PYR concentration groups, with the high PYR concentration treatment group requiring more SOD to counter ROS production than that under low PYR concentration treatment. Notably, the SOD value of PYR_8 + PS increased by 1.27-fold significantly compared with PYR alone in the high PYR concentration treatment group. Additionally, MDA and LDH levels reflected lipid peroxidation in the cell membrane of *M. aeruginosa* (Bailly et al., 1996; Jeng and Swanson, 2006; Zhu et al., 2019), which showed similar trends to ROS and SOD values. PYR_8 + PS significantly increased the MDA and LDH values of *M. aeruginosa* compared to PYR_8 alone, by 1.45 and 2.25-fold, respectively (Fig. 2g-h).

Poisoning effect of pollutants on algal cells was used to be initiated from the production of ROS within these cells, while the algae own antioxidant system also generated enzymes as defenses against oxidative harm, with SOD being the paramount antioxidant enzyme (Ighodaro and Akinloye, 2018). Furthermore, MDA and LDH were indicative of the cell membrane damage under ROS attack (Huang et al., 2022). In the treatment of only PYR, algal cell breakage was observed, a result of ROS overproduction instigated by allelochemicals that destroyed cell wall structures and membrane integrity (Lu et al., 2016), leading to leaks of electrolytes, nucleic acids, and proteins from the cells (Zhang et al., 2010). Our study also showed an increase in ROS and antioxidant enzyme contents in algal cells subjected to PYR alone in comparison to the CK. After introducing PS-MPs, the cell membrane became more permeable, potentially because 1 μm PS-MPs would aggregate and adhere to algal cell surfaces (Cao et al., 2022; Song et al., 2023), thereby decreasing membrane fluidity and interrupting the exchange of substances and energy flow between the cells and their surroundings (Liu et al., 2020). MPs were demonstrated to induce ROS generation in algal cells, subsequently causing membrane injury (Zheng et al., 2021b). In high concentration treatments, the significant rise in MDA and LDH levels in algal cells post the introduction of PS-MPs, as opposed to those treated with 8 mg/L PYR only, signified damage to the cell membrane caused by PS-MPs (Li et al., 2022). These discoveries implied that the suppressive actions of PS-MPs and PYR on algal cells possibly resulted from a combined effect of membrane damage and oxidative stress, a perspective also validated by Wang et al. (2023a).

3.3. MCs synthesis and release

The intensification of cyanobacteria bloom has been linked to a consequential outcome, the prolific synthesis of MCs, which posed a significant threat to the safety of drinking water (Dai et al., 2016). As

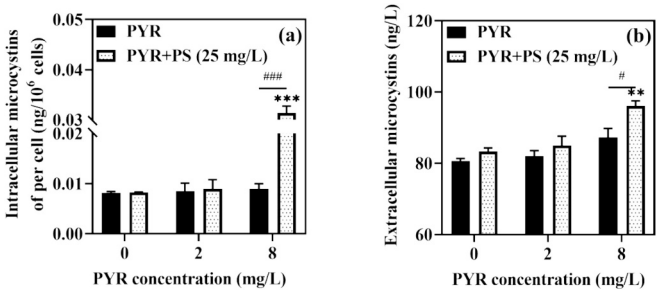

Fig. 3. Intracellular MCs of per cell (intra-MCs) (a) and extracellular MCs (extra-MCs) (b) of *M. aeruginosa* under individual and combined exposure experiments after 7 days. Data were expressed as the mean ± SD. Significant differences between the control and treatments were indicated by asterisks (*), with the levels of significance denoted as $*p < 0.05$, $**p < 0.01$ and $***p < 0.001$. Horizontal lines with a pound (#) represented significant differences between the only PYR treatment and their combined treatments with PS-MPs, $\#p < 0.05$, $\#\#p < 0.01$, $\#\#\#p < 0.001$.

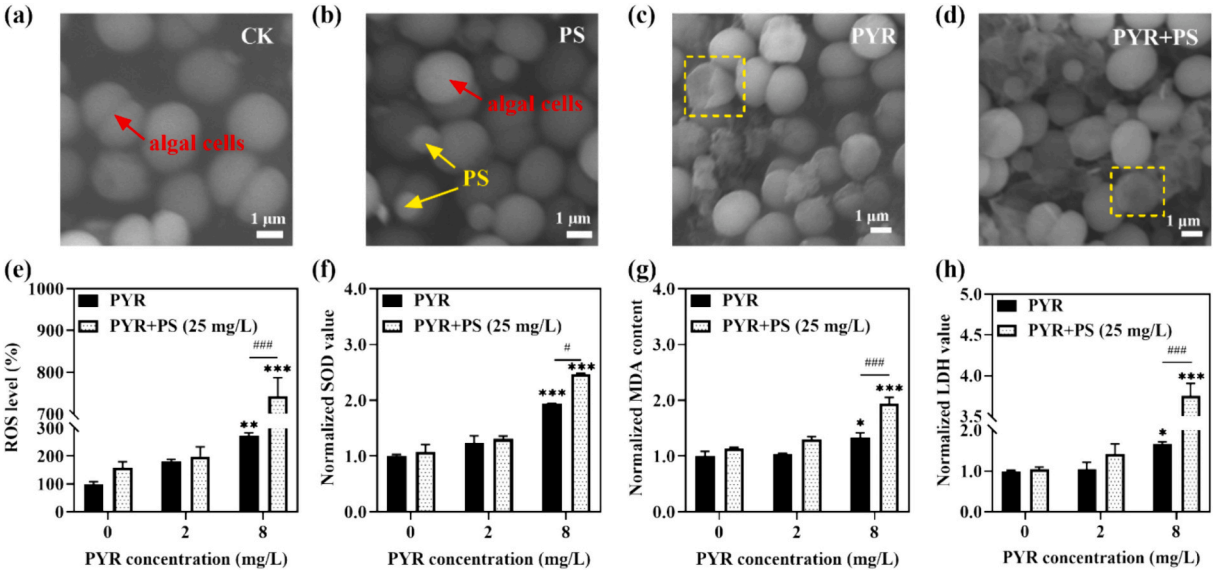

Fig. 2. The effects of individual and combined exposure experiments on *M. aeruginosa* were assessed through SEM images (a-d) and ROS level, SOD value, MDA content and LDH value (e-h). PS-MPs in the images were identified by yellow arrows, red arrows denoted algal cells, and impaired cells were highlighted with yellow frames. Data were expressed as the mean ± SD. Significant differences between the control and treatments were indicated by asterisks (*), with the levels of significance denoted as $*p < 0.05$, $**p < 0.01$ and $***p < 0.001$. Horizontal lines with a pound (#) represented significant differences between the only PYR treatment and their combined treatments with PS-MPs, $\#p < 0.05$, $\#\#p < 0.01$, $\#\#\#p < 0.001$.

illustrated in Fig. 3a-b, intra-MCs and extra-MCs were measured under individual and combined exposure treatments after 7 days. Only PS + PYR 8 showed significantly higher performance than CK. Specifically, intra-MCs in PYR_8 + PS were 3.88-fold higher than that in CK ($p < 0.05$), and extra-MCs were 1.19-fold higher than that in CK ($p < 0.05$). Moreover, within the high concentration treatment group, intra-MCs in PYR_8 + PS were 3.49-fold higher than that in PYR_8 ($p < 0.05$), and extra-MCs were 1.10-fold higher than that in PYR_8 ($p < 0.05$). These findings indicated that the addition of PS-MPs significantly influenced the synthesis and release of MCs of *M. aeruginosa* under high PYR concentration.

Analyzing intra-MCs facilitated the understanding of the algal cells physiological processes and metabolic activities before their release into the surrounding environment (Leflaive and Ten-Hage, 2007). Conversely, extra-MCs were discharged into the water, exerting adverse effects on the ecosystem and drinking water safety (Li et al., 2020b). Notably, it is crucial to acknowledge the existence of a certain association between intra-MCs and extra-MCs (Wu et al., 2021). By augmenting the levels of intra-MCs, algal cells protected themselves from ROS damage (Zilliges et al., 2011; Feng et al., 2020). Zheng et al. (2021a) proposed that MCs derived from the algal cells could potentially serve as a protective mechanism against oxidative stress, as the algal cells resorted to alternative coping mechanisms when the SOD activity was inhibited. The synthesis of MCs was interpreted as a defensive response of algal cells against external stress (Wu et al., 2021). Moreover, Feng et al. (2020) attributed the stimulated synthesis of MCs to membrane damage and the up-regulation of biological transport proteins. PS-MPs and PYR regulated the synthesis and release of MCs by influencing gene expression in the algal cells (Zheng et al., 2021a). Zhang et al. (2023) suggested that combined stress from MPs and boron enhances the transcriptional synthesis of MCs. Shao et al. (2009) observed a slight up-regulation of the *mcyB* gene, responsible for MCs synthesis, in the algal cells exposed to 4 mg/L of PYR. While the introduction of PS-MPs aided allelochemicals in eliminating toxic *Microcystis*, our data indicated a concurrent increase in the release of MCs. This suggested the persistence of significant ecological risks associated with PS-MPs, thereby necessitating the exploration of appropriate strategies to manage the extensive release of MCs. In summary, PS-MPs and PYR induced oxidative stress in *M. aeruginosa*, resulting in cell membrane damage and gene transcription regulation, which further contributed to a substantial synthesis and release of MCs, ultimately impacting ecological security. In light of these findings, prudent considerations should be given to the safe removal of MCs and the potential reciprocal impact of MCs on MPs.

3.4. GHGs emissions

As depicted in Fig. 4a-c, the emission of CO_2 by *M. aeruginosa* was approximately thousand-fold greater than that of N_2O and CH_4, underscoring the predominant role of CO_2 as the primary GHGs released by *M. aeruginosa*. The emission rates of CO_2, N_2O and CH_4 by *M. aeruginosa* exhibited a gradual decrease throughout the culture process under CK, PS-MPs, and low PYR concentration treatment group. Notably, on day 5 and 7, no significant differences were observed among these four treatments. Conversely, the high PYR concentration treatment group increased the GHGs emission rates of significantly. Specifically, the CO_2 and N_2O emission rates of PYR_8 + PS reached their maximum at day 5 (maximum: 43.56 and 0.22 μg/(10^6 cells)/h, respectively) and declined thereafter. On the contrary, the emission rates of CH_4 in PYR_8 + PS exhibited a fluctuating pattern of gradual decline, followed by a subsequent rise, and then another decline during the culture period, displaying significant volatility and instability. In addition, the emission rates of GHGs after adding PS-MPs were always significantly higher than those without adding PS-MPs in the high PYR concentration treatment group. PYR_8 + PS exhibited significantly higher emission rates of CO_2, N_2O and CH_4 compared to PYR_8, with respective increases of 2.66, 2.23 and 2.17-fold ($p < 0.05$) after 7 days. It proves that PS-MPs have a strong

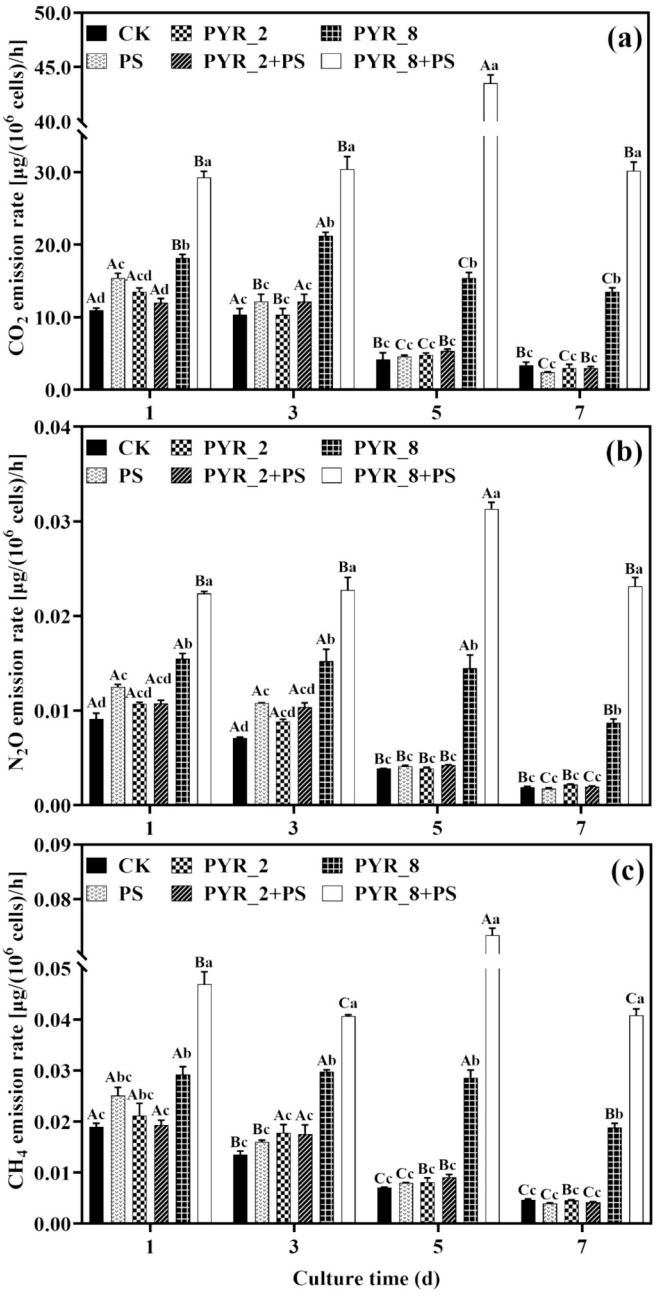

Fig. 4. The GHGs (CO_2 (a), N_2O (b) and CH_4 (c)) emission rates of *M. aeruginosa* under individual and combined exposure experiments at incubation durations of 1, 3, 5 and 7 days. Data were presented as the mean ± SD; and treatments labeled with different letters exhibited significant differences ($p < 0.05$). Capital letters denote significant differences in the same treatment across various culture times ($p < 0.05$). Lowercase letters indicate the significant difference between different treatments at the same culture time ($p < 0.05$).

effect on GHGs emissions of *M. aeruginosa* under high PYR concentration. The downward trend of GHGs emission rates in the low PYR concentration treatment group can be attributed to the gradual depletion of nutrients and the growth of algae, while the flattening of emission rates in the later period may be attributed to the resilience of the algae cells themselves, allowing them to overcome slight external pressures and return to normal growth (Taghizadeh et al., 2020). In the high PYR concentration treatment group, the addition of PS-MPs resulted in significant inhibition of photosynthesis, oxidative stress-induced cell membrane damage and DNA structural disruption of *M. aeruginosa*.

These environmental stressors prompted *M. aeruginosa* to initiate growth restoration mechanisms, including the synthesis of proteins (such as SOD, MDA, LDH and MCs) and DNA replication(Sabatini et al., 2009; Kaur et al., 2019). During the synthesis of these compounds, intracellular organic matter decomposition was required to provide the necessary energy (Feng et al., 2023), inevitably leading to the release of corresponding metabolites, including CO_2, N_2O and CH_4 (Pelroy et al., 1972; Fabisik et al., 2022). This might account for the substantial increase in the emission rates of GHGs following the addition of PS-MPs upon a foundation of high PYR concentration. However, it should be noted that the culture time in this study was limited to 7 days, and longer culture duration and more extensive observations would yield a deeper understanding of the effects of PS-MPs and PYR on the GHGs emissions of *M. aeruginosa*.

3.5. Differentially expressed gene analysis

Transcriptomic analysis was conducted to gain deeper insights into the impact of PS-MPs and PYR on *M. aeruginosa*. Remarkably, our analysis revealed that PS-MPs exerted more pronounced effects in the high PYR concentration treatment group. Consequently, we focused our transcriptome examination exclusively on this high PYR concentration treatment group. Our samples exhibited quality metrics, including Q20, Q30 and genome mapped ratio, all exceeding 95 % (Table S1), indicating their high quality and strong similarity to reference genome comparisons, making them suitable for subsequent transcriptome analysis. The results for differentially expressed genes (DEGs) between experimental groups were summarized in Table S2. It should be noted that the PYR_PS and PYR comparison revealed 1119 DEGs, comprising 328 DEGs demonstrating up-regulation and 791 DEGs manifesting down-regulation. It was evident that the addition of PS-MPs significantly affected the gene expression of *M. aeruginosa*, in contrast to the treatment with only PYR.

Subsequently, we conducted GO functional enrichment analysis on *M. aeruginosa* under the PYR treatment (Fig. 5a) and PYR + PS treatment (Fig. 5b) with chordal graphs. It could be seen from these terms that DNA synthesis, membrane structure, catalytic activity of some enzymes inside the cell and other functions of *M. aeruginosa* were affected under

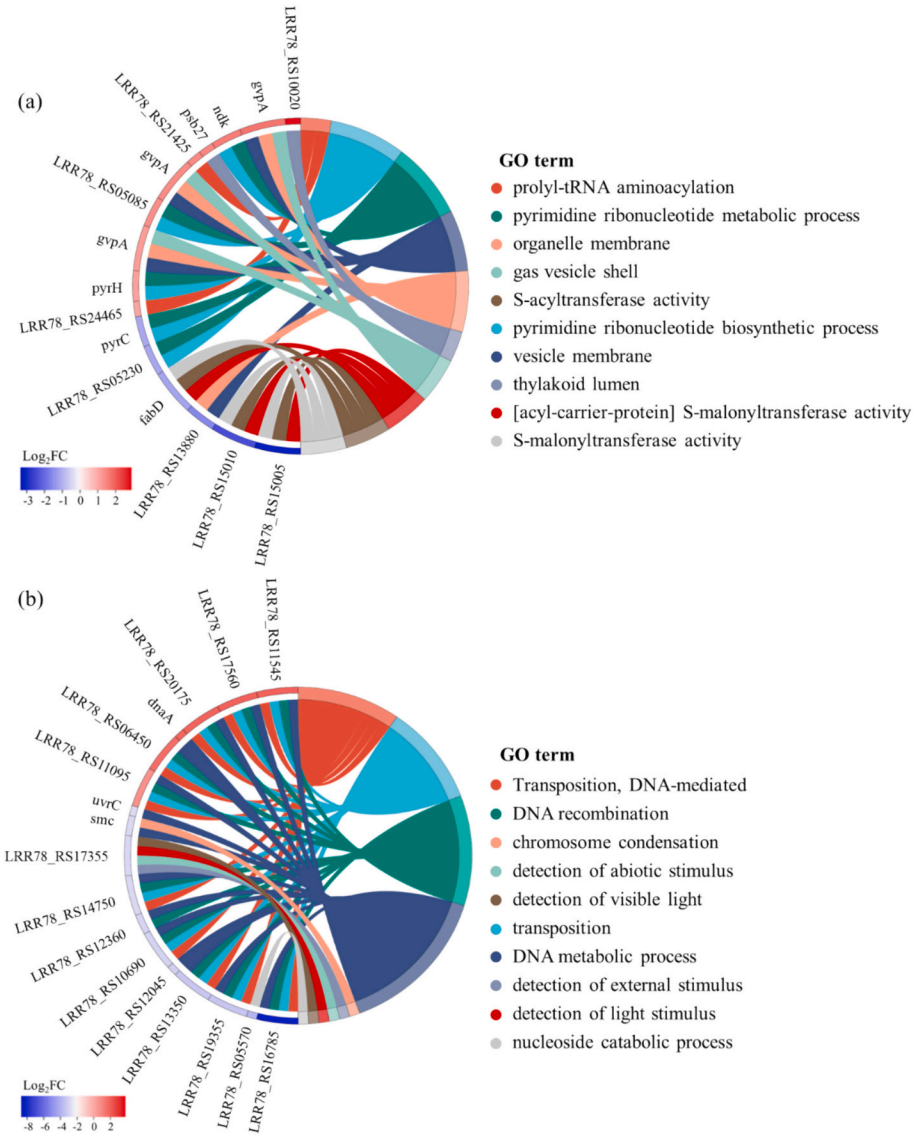

Fig. 5. GO functional enrichment chordal graphs. GO functional enrichment chordal graphs of *M. aeruginosa* under PYR treatment (a) and PYR + PS treatment (b). The GO functional enrichment chordal graphs represented the top ten with the most enriched terms. Genes enriched for these GO functions were ordered by Log_2FC ($Log_2FC > 0$ showed up-regulated, $Log_2FC < 0$ showed down-regulated). Higher $|log_2FC|$ values indicated larger differential expression multiples of the genes, while values closer to 0 indicated smaller differential expression multiples of the genes.

PYR treatment in Fig. 5a. The process of "pyrimidine ribonucleotide biosynthetic process" and "pyrimidine ribonucleotide metabolic process" contained the largest number of genes, indicating an impact on ribonucleotide production (Yang et al., 2021). The down-regulation of genes associated with "[acyl-carrier-protein] S-malonyltransferase activity," "S-acyltransferase activity," and "S-malonyltransferase activity" suggested inhibition of fatty acid synthesis and enzyme activity (Sung et al., 2013). As can be seen from Fig. 5b, DNA synthesis and light detection of *M. aeruginosa* were affected in PYR + PS treatment. The process of "DNA metabolic process" contained the largest number of genes, with over half of them being down-regulated. This implied that the biological activity of DNA was influenced under PYR + PS treatment (Duan et al., 2022). Genes associated with "Detection of abiotic stimulus", "Detection of external stimulus", "Detection of light stimulus", "Detection of visible light", "Nucleoside catabolic process" and "Chromosome condensation" were down-regulated, indicating inhibition of biological activities such as stimulus detection and cell division of *M. aeruginosa* (Hu et al., 2018).

In addition, we screened the genes related to MCs synthesis and conducted heat map analysis (Fig. 6). The genes involved in the synthesis of MCs primarily consist of those encoding non-ribosomal peptide synthetases (such as *mcyA*, *mcyB*, *mcyC*, *mcyD* and *mcyE*) and several modified auxiliary genes (such as *mcyG*, *mcyI* and *mcyJ*) (Qu et al., 2018). The genes related to MCs were up-regulated under the PYR treatment and PYR + PS treatment. In the PYR + PS treatment, the Log_2FC values of *mcyA*, *mcyD*, *mcyE*, *mcyI*, *mcyJ* genes showed higher up-regulation compared to the PYR treatment. However, the expression of *mcyC* was down-regulated in the PYR + PS treatment. Gene *mcyC* is a peptide synthetase that contains an integrated thioesterase domain responsible for catalyzing the final step in MCs biosynthesis. The down-regulation of *mcyC* suggested a decrease in MCs synthesis (Yu et al., 2023). This was different from the expression of other genes and deserved attention. Notably, the expression of *mcyJ* displayed a significant up-regulation by 1.23 Log_2FC in the PYR_PS treatment. Gene *mcyJ* was involved in the modification and transport of MCs (Harke and Gobler, 2015) and played a critical role in *O*-methylation (Tillett et al., 2000). This implied that the presence of PS-MPs and PYR promoted the synthesis of MCs by *M. aeruginosa*. Li et al. (2023) supported this notion in their research.

Moreover, genes related to the GHGs (CO_2, N_2O and CH_4) were also screened for heat map analysis (Fig. 6). We investigated the analysis of genes related to carbon metabolism, nitrogen metabolism and methane metabolism affecting GHGs release of *M. aeruginosa* under the PYR and PYR + PS treatment. The majority of genes affecting the release of CO_2, N_2O and CH_4 exhibited down-regulation in the PYR treatment. Specifically, the *accA*, *accD*, *pckA* and *por* genes, which were associated with CO_2 release, showed significant down-regulation with Log_2FC values of −1.11, −1.20, −1.32 and −1.14, respectively. Additionally, the *cysK* and *narB* genes, involving in N_2O release, displayed significant down-regulation with Log_2FC values of −1.54 and −1.40, respectively. This result diverged from that observed in Section 3.4, where it was shown that under only PYR treatment, GHGs emissions increased, whereas in this section, expression of genes related to GHGs was found to be down-regulated instead. We speculated that this discrepancy might have arisen due to other genes promoting GHGs production through compensatory mechanisms (El-Brolosy and Stainier, 2017). The precise reasons underlying this discrepancy warrant further investigation in future studies. However, the expression of many genes was up-regulated in the PYR + PS treatment. Notably, the *cynT*, *cysA* and *cysW* genes, related to N_2O release, exhibited significant up-regulation with Log_2FC values of 1.07, 1.03 and 1.85, respectively. In addition, there were also some genes that have been commonly studied related to N_2O emission, such as *hcp* gene encoding hybrid cluster protein (Wang et al., 2016b) and *nirA* gene encoding nitrite reductase (Ma et al., 2023). There were also *nrtA*, *nrtB*, *nrtC* and *nrtD* genes involved in the nitrogen cycle, all of which were related to nitrous oxide metabolism and emission (Wang et al., 2021b). Moreover, the expression of these genes was up-regulated under PYR + PS treatment. The genes *accA* and *accD* encoded acetyl-CoA carboxylase (Lee et al., 2012; Song et al., 2013), while *pckA* and *por* were involved in CO_2 fixation (Inui et al., 1999; Bergauer et al., 2013; He et al., 2013). The significant down-regulation of these genes indicated a decrease in CO_2 fixation. Moreover, the down-regulation of *narB*, which encoded nitrate reductase (Hidalgo-García et al., 2019; Li et al., 2020c), suggesting an ineffective reduction of nitrate.

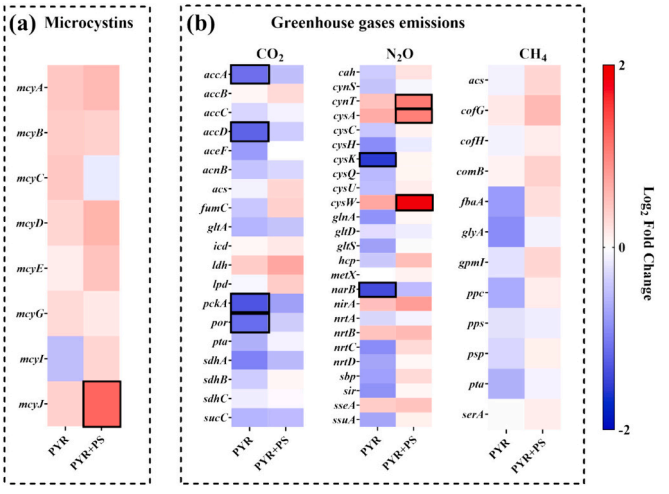

Fig. 6. Heat maps of gene expression associated with MCs synthesis (a) and GHGs emissions (b) under PYR treatment and PYR + PS treatment. $Log_2FC > 0$ showed up-regulated, $Log_2FC < 0$ showed down-regulated. Higher $|log_2FC|$ values indicated larger differential expression multiples of the genes, while values closer to 0 indicated smaller differential expression multiples of the genes. The black frames indicated a significant difference of the genes. (significant difference threshold: *p*-adjust <0.001 & $|log_2FC| \geq 1$).

4. Conclusion

This study investigated the impact of PS-MPs on the allelopathy of PYR on *M. aeruginosa*. The outcomes revealed that PS-MPs significantly potentiated the inhibition of high PYR concentration on the growth and photosynthesis of *M. aeruginosa*, leading to a remarkable increase in antioxidant enzyme activity, MCs release, and GHGs emission rates. Conversely, the effects were not significant at low PYR concentration. In addition, transcriptomic analysis showed that PS-MPs and PYR led to the dysregulation of gene expression related to DNA synthesis, membrane function, enzyme activity, stimulus detection, MCs release and GHGs emissions in *M. aeruginosa*. The possible toxic mechanisms were that PYR and PS-MPs induced ROS production in algal cells, damaging cell membranes and disrupting photosynthesis, which led to an increased release of MCs and GHGs emissions. Specifically, PS-MPs accumulated and sticked to the cell surface, weakening membrane fluidity and hindering light reception, further suppressing photosynthesis, exacerbating cellular damage and enhancing the release of MCs and GHGs emissions. This conclusion underscores the significance and potential ecological implications of MPs in freshwater environments, providing a reference for further research on the ecological risk assessment of MPs in freshwater ecosystems.

CRediT authorship contribution statement

Linqing Du: Writing – original draft, Visualization, Conceptualization. **Qinglong Liu:** Writing – review & editing. **Lan Wang:** Writing – review & editing. **Honghong Lyu:** Writing – review & editing. **Jingchun Tang:** Writing – review & editing, Supervision, Resources.

Declaration of competing interest

The authors declare that they have no known competing financial interests or personal relationships that could have appeared to influence the work reported in this paper.

Data availability

Data will be made available on request.

Acknowledgments

National Natural Science Foundation of China (42377225, U1806216), Key Research and Development Program of Tianjin (23YFXTHZ00170), and 111 program, Ministry of Education, China (B17025).

Appendix A. Supplementary data

Supplementary data to this article can be found online at https://doi.org/10.1016/j.scitotenv.2024.173864.

References

Amaneesh, C., Anna Balan, S., Silpa, P.S., Kim, J.W., Greeshma, K., Aswathi Mohan, A., Robert Antony, A., Grossart, H.-P., Kim, H.-S., Ramanan, R., 2023. Gross negligence: impacts of microplastics and plastic leachates on phytoplankton community and ecosystem dynamics. Environ. Sci. Technol. 57, 5–24. https://doi.org/10.1021/acs.est.2c05817.

Bailly, C., Benamar, A., Corbineau, F., Come, D., 1996. Changes in malondialdehyde content and in superoxide dismutase, catalase and glutathione reductase activities in sunflower seeds as related to deterioration during accelerated aging. Physiol. Plant. 97, 104–110. https://doi.org/10.1111/j.1399-3054.1996.tb00485.x.

Barnes, S.J., 2019. Understanding plastics pollution: the role of economic development and technological research. Environ. Pollut. 249, 812–821. https://doi.org/10.1016/j.envpol.2019.03.108.

Bergauer, K., Sintes, E., van Bleijswijk, J., Witte, H., Herndl, G.J., 2013. Abundance and distribution of archaeal acetyl-CoA/propionyl-CoA carboxylase genes indicative for putatively chemoautotrophic Archaea in the tropical Atlantic's interior. FEMS Microbiol. Ecol. 84, 461–473. https://doi.org/10.1111/1574-6941.12073.

Bhattacharya, P., Lin, S., Turner, J.P., Ke, P.C., 2010. Physical adsorption of charged plastic nanoparticles affects algal photosynthesis. J. Phys. Chem. C 114, 16556–16561. https://doi.org/10.1021/jp1054759.

Cao, Q., Sun, W., Yang, T., Zhu, Z., Jiang, Y., Hu, W., Wei, W., Zhang, Y., Yang, H., 2022. The toxic effects of polystyrene microplastics on freshwater algae Chlorella pyrenoidosa depends on the different size of polystyrene microplastics. Chemosphere 308, 136135. https://doi.org/10.1016/j.chemosphere.2022.136135.

Chen, Y., Ling, Y., Li, X., Hu, J., Cao, C., He, D., 2020. Size-dependent cellular internalization and effects of polystyrene microplastics in microalgae P. helgolandica var. tsingtaoensis and S. quadricauda. J. Hazard. Mater. 399, 123092 https://doi.org/10.1016/j.jhazmat.2020.123092.

Dai, R., Wang, P., Jia, P., Zhang, Y., Chu, X., Wang, Y., 2016. A review on factors affecting microcystins production by algae in aquatic environments. World J. Microbiol. Biotechnol. 32, 51. https://doi.org/10.1007/s11274-015-2003-2.

Duan, C., Yao, L., Lv, J.-H., Jia, C.-W., Tian, F.-H., Li, C.-T., 2022. Systematic analysis of changes across different developmental stages of the mushroom Sarcomyxa edulis. Gene 824, 146450. https://doi.org/10.1016/j.gene.2022.146450.

Dziga, D., Suda, M., Bialczyk, J., Czaja-Prokop, U., Lechowski, Z., 2007. The alteration of Microcystis aeruginosa biomass and dissolved microcystin-LR concentration following exposure to plant-producing phenols. Environ. Toxicol. 22, 341–346. https://doi.org/10.1002/tox.20276.

El-Brolosy, M.A., Stainier, D.Y.R., 2017. Genetic compensation: a phenomenon in search of mechanisms. PLoS Genet. 13, e1006780 https://doi.org/10.1371/journal.pgen.1006780.

Fabisik, F., Guieysse, B., Procter, J., Plouviez, M.J.E., 2022. Nitrous oxide (N 2 O) synthesis by Microcystis aeruginosa. EGUsphere [preprint] 1-12. https://doi.org/10.5194/egusphere-2022-1153.

Feng, L.-J., Sun, X.-D., Zhu, F.-P., Feng, Y., Duan, J.-L., Xiao, F., Li, X.-Y., Shi, Y., Wang, Q., Sun, J.-W., Liu, X.-Y., Liu, J.-Q., Zhou, L.-L., Wang, S.-G., Ding, Z., Tian, H., Galloway, T.S., Yuan, X.-Z., 2020. Nanoplastics promote microcystin synthesis and release from cyanobacterial Microcystis aeruginosa. Environ. Sci. Technol. 54, 3386–3394. https://doi.org/10.1021/acs.est.9b06085.

Feng, L., Jia, D., Wang, Z., Guo, J., Zou, X., Rao, M., Kuang, C., Ye, J., Chen, C., Cheng, J., 2023. FIB-SEM combined with proteomics and modification omics clarified mechanisms of lipids synthesis in organelles of Chlorella pyrenoidosa cells with high CO2 concentration. Sci. Total Environ. 891, 164516 https://doi.org/10.1016/j.scitotenv.2023.164516.

Gao, Y., Lu, J., Orr, P.T., Chuang, A., Franklin, H.M., Burford, M.A., 2020. Enhanced resistance of co-existing toxigenic and non-toxigenic Microcystis aeruginosa to pyrogallol compared with monostrains. Toxicon 176, 47–54. https://doi.org/10.1016/j.toxicon.2020.01.013.

Harke, M.J., Gobler, C.J., 2015. Daily transcriptome changes reveal the role of nitrogen in controlling microcystin synthesis and nutrient transport in the toxic cyanobacterium, *Microcystis aeruginosa*. BMC Genomics 16, 1068. https://doi.org/10.1186/s12864-015-2275-9.

He, P., Liu, Y., Yue, W., Huang, X., 2013. Key genes expression of reductive tricarboxylic acid cycle from deep-sea hydrothermal chemolithoautotrophic Caminibacter profundus in response to salinity, pH and O2. Acta Oceanol. Sin. 32, 35–41. https://doi.org/10.1007/s13131-013-0275-7.

Hidalgo-García, A., Torres, M.J., Salas, A., Bedmar, E.J., Girard, L., Delgado, M.J., 2019. Rhizobium etli produces nitrous oxide by coupling the assimilatory and denitrification pathways. Front. Microbiol. 10 https://doi.org/10.3389/fmicb.2019.00980.

Hou, X., Mu, L., Hu, X., Guo, S., 2023. Warming and microplastic pollution shape the carbon and nitrogen cycles of algae. J. Hazard. Mater. 447, 130775 https://doi.org/10.1016/j.jhazmat.2023.130775.

Hu, X., Ke, L., Wang, Z., Zeng, Z., 2018. Dynamic transcriptome landscape of Asian domestic honeybee (Apis cerana) embryonic development revealed by high-quality RNA sequencing. BMC Dev. Biol. 18, 11. https://doi.org/10.1186/s12861-018-0169-1.

Huang, S., Zhang, B., Liu, Y., Feng, X., Shi, W., 2022. Revealing the influencing mechanisms of polystyrene microplastics (MPs) on the performance and stability of the algal-bacterial granular sludge. Bioresour. Technol. 354, 127202 https://doi.org/10.1016/j.biortech.2022.127202.

Ighodaro, O.M., Akinloye, O.A., 2018. First line defence antioxidants-superoxide dismutase (SOD), catalase (CAT) and glutathione peroxidase (GPX): their fundamental role in the entire antioxidant defence grid. Alexandria Journal of Medicine 54, 287–293. https://doi.org/10.1016/j.ajme.2017.09.001.

Inui, M., Nakata, K., Roh, J.H., Zahn, K., Yukawa, H., 1999. Molecular and functional characterization of the Rhodopseudomonas palustris no. 7 phosphoenolpyruvate carboxykinase gene. J. Bacteriol. 181, 2689–2696. https://doi.org/10.1128/jb.181.9.2689-2696.1999.

Jambeck, J.R., Geyer, R., Wilcox, C., Siegler, T.R., Perryman, M., Andrady, A., Narayan, R., Law, K.L., 2015. Plastic Waste Inputs from Land into the Ocean, 347, pp. 768–771. https://doi.org/10.1126/science.1260352.

Jeng, H.A., Swanson, J., 2006. Toxicity of metal oxide nanoparticles in mammalian cells. J. Environ. Sci. Health A 41, 2699–2711. https://doi.org/10.1080/10934520600966177.

Jin, Z., Du, L., Cheng, Q., Jiang, Y., Hui, C., Xu, L., Zhao, Y., Jiang, H., 2022. Physiological and transcriptional responses of Dictyosphaerium sp. under co-exposure of a typical microplastic and nonylphenol. Environ. Res. 204, 112287 https://doi.org/10.1016/j.envres.2021.112287.

Kaur, S., Srivastava, A., Kumar, S., Srivastava, V., Ahluwalia, A.S., Mishra, Y., 2019. Biochemical and proteomic analysis reveals oxidative stress tolerance strategies of Scenedesmus abundans against allelochemicals released by Microcystis aeruginosa. Algal Res. 41, 101525 https://doi.org/10.1016/j.algal.2019.101525.

Kaur, M., Saini, K.C., Ojah, H., Sahoo, R., Gupta, K., Kumar, A., Bast, F., 2022. Abiotic stress in algae: response, signaling and transgenic approaches. J. Appl. Phycol. 34, 1843–1869. https://doi.org/10.1007/s10811-022-02746-7.

Laskar, N., Kumar, U., 2019. Plastics and microplastics: a threat to environment. Environ. Technol. Innov. 14, 100352 https://doi.org/10.1016/j.eti.2019.100352.

Lee, S., Jeon, E., Jung, Y., Lee, J., 2012. Heterologous co-expression of accA, fabD, and thioesterase genes for improving long-chain fatty acid production in Pseudomonas aeruginosa and Escherichia coli. Appl. Biochem. Biotechnol. 167, 24–38. https://doi.org/10.1007/s12010-012-9644-5.

Leflaive, J.P., Ten-Hage, L., 2007. Algal and cyanobacterial secondary metabolites in freshwaters: a comparison of allelopathic compounds and toxins. Freshw. Biol. 52, 199–214. https://doi.org/10.1111/j.1365-2427.2006.01689.x.

Li, S., Wang, P., Zhang, C., Zhou, X., Yin, Z., Hu, T., Hu, D., Liu, C., Zhu, L., 2020a. Influence of polystyrene microplastics on the growth, photosynthetic efficiency and aggregation of freshwater microalgae Chlamydomonas reinhardtii. Sci. Total Environ. 714, 136767 https://doi.org/10.1016/j.scitotenv.2020.136767.

Li, X., Chen, S., Zeng, J., Chabi, K., Song, W., Xian, X., Yu, X., 2020b. Impact of chlorination on cell inactivation, toxin release and degradation of cyanobacteria of development and maintenance stage. Chem. Eng. J. 397, 125378 https://doi.org/10.1016/j.cej.2020.125378.

Li, X., Qiao, J., Li, S., Häggblom, M.M., Li, F., Hu, M., 2020c. Bacterial communities and functional genes stimulated during anaerobic arsenite oxidation and nitrate reduction in a paddy soil. Environ. Sci. Technol. 54, 2172–2181. https://doi.org/10.1021/acs.est.9b04308.

Li, X., Luo, J., Zeng, H., Zhu, L., Lu, X., 2022. Microplastics decrease the toxicity of sulfamethoxazole to marine algae (Skeletonema costatum) at the cellular and molecular levels. Sci. Total Environ. 824, 153855 https://doi.org/10.1016/j.scitotenv.2022.153855.

Li, Z., An, L., Yan, F., Shen, W., Du, W., Dai, R., 2023. Evaluation of the effects of different phosphorus sources on Microcystis aeruginosa growth and microcystin production via transcriptomic surveys. Water 15, 1938. https://doi.org/10.3390/w15101938.

Liu, B.-Y., Zhou, P.-J., Tian, J.-R., Jiang, S.-Y., 2007. Effect of pyrogallol on the growth and pigment content of cyanobacteria-blooming toxic and nontoxic *Microcystis aeruginosa*. Bull. Environ. Contam. Toxicol. 78, 499–502. https://doi.org/10.1007/s00128-007-9096-8.

Liu, G., Jiang, R., You, J., Muir, D.C.G., Zeng, E.Y., 2020. Microplastic impacts on microalgae growth: effects of size and humic acid. Environ. Sci. Technol. 54, 1782–1789. https://doi.org/10.1021/acs.est.9b06187.

Liu, Z., Tang, J., Ren, X., Schaeffer, S.M., 2021. Effects of phosphorus modified nZVI-biochar composite on emission of greenhouse gases and changes of microbial community in soil. Environ. Pollut. 274, 116483 https://doi.org/10.1016/j.envpol.2021.116483.

Liu, X., Ma, J., Guo, S., Shi, Q., Tang, J., 2022a. The combined effects of nanoplastics and dibutyl phthalate on Streptomyces coelicolor M145. Sci. Total Environ. 826, 154151 https://doi.org/10.1016/j.scitotenv.2022.154151.

Liu, Y., Shi, Q., Liu, X., Wang, L., He, Y., Tang, J., 2022b. Perfluorooctane sulfonate (PFOS) enhanced polystyrene particles uptake by human colon adenocarcinoma Caco-2 cells. Sci. Total Environ. 848, 157640 https://doi.org/10.1016/j.scitotenv.2022.157640.

Liu, Y., Jin, T., Wang, L., Tang, J., 2023. Polystyrene micro and nanoplastics attenuated the bioavailability and toxic effects of Perfluorooctane sulfonate (PFOS) on soybean (Glycine max) sprouts. J. Hazard. Mater. 448, 130911 https://doi.org/10.1016/j.jhazmat.2023.130911.

Lu, Z., Zhang, Y., Gao, Y., Liu, B., Sun, X., He, F., Zhou, Q., Wu, Z., 2016. Effects of pyrogallic acid on Microcystis aeruginosa: oxidative stress related toxicity. Ecotoxicol. Environ. Saf. 132, 413–419. https://doi.org/10.1016/j.ecoenv.2016.06.039.

Ma, L., Li, Z., Liu, G., Liu, W., 2023. Low-level cadmium alleviates the disturbance of doxycycline on nitrogen removal and N2O emissions in ditch wetlands by altering microbial community and enzymatic activity. J. Clean. Prod. 387, 135807 https://doi.org/10.1016/j.jclepro.2022.135807.

Mao, Y., Ai, H., Chen, Y., Zhang, Z., Zeng, P., Kang, L., Li, W., Gu, W., He, Q., Li, H., 2018. Phytoplankton response to polystyrene microplastics: perspective from an entire growth period. Chemosphere 208, 59–68. https://doi.org/10.1016/j.chemosphere.2018.05.170.

Miles, C.O., Sandvik, M., Nonga, H.E., Rundberget, T., Wilkins, A.L., Rise, F., Ballot, A., 2012. Thiol derivatization for LC-MS identification of microcystins in complex matrices. Environ. Sci. Technol. 46, 8937–8944. https://doi.org/10.1021/es301808h.

Nakai, S., Inoue, Y., Hosomi, M., Murakami, A., 2000. Myriophyllum spicatum-released allelopathic polyphenols inhibiting growth of blue-green algae Microcystis aeruginosa. Water Res. 34, 3026–3032. https://doi.org/10.1016/S0043-1354(00)00039-7.

Nakai, S., Inoue, Y., Hosomi, M., 2001. Algal growth inhibition effects and inducement modes by plant-producing phenols. Water Res. 35, 1855–1859. https://doi.org/10.1016/s0043-1354(00)00444-9.

Pelroy, R.A., Rippka, R., Stanier, R.Y., 1972. Metabolism of glucose by unicellular blue-green algae. Arch. Mikrobiol. 87, 303–322. https://doi.org/10.1007/BF00409131.

Plaas, H.E., Paerl, H.W., 2021. Toxic cyanobacteria: a growing threat to water and air quality. Environ. Sci. Technol. 55, 44–64. https://doi.org/10.1021/acs.est.0c06653.

Qiao, R., Lu, K., Deng, Y., Ren, H., Zhang, Y., 2019. Combined effects of polystyrene microplastics and natural organic matter on the accumulation and toxicity of copper in zebrafish. Sci. Total Environ. 682, 128–137. https://doi.org/10.1016/j.scitotenv.2019.05.163.

Qu, J., Shen, L., Zhao, M., Li, W., Jia, C., Zhu, H., Zhang, Q., 2018. Determination of the role of Microcystis aeruginosa in toxin generation based on phosphoproteomic profiles. Toxins (Basel) 10, 304. https://doi.org/10.3390/toxins10070304.

Ren, X., Tang, J., Liu, X., Liu, Q., 2020. Effects of microplastics on greenhouse gas emissions and the microbial community in fertilized soil. Environ. Pollut. 256, 113347 https://doi.org/10.1016/j.envpol.2019.113347.

Sabatini, S.E., Juárez, Á.B., Eppis, M.R., Bianchi, L., Luquet, C.M., Ríos de Molina, M.d. C., 2009. Oxidative stress and antioxidant defenses in two green microalgae exposed to copper. Ecotoxicol. Environ. Saf. 72, 1200–1206. https://doi.org/10.1016/j.ecoenv.2009.01.003.

Shan, W., Xiao-hong, L., Long, Y., 2011. The effect of O-dihydroxybenzene and pyrogallol on the chlorella pyrenoidosa chick growing. Procedia Environ. Sci. 11, 1459–1464. https://doi.org/10.1016/j.proenv.2011.12.219.

Shao, J., Wu, Z., Yu, G., Peng, X., Li, R., 2009. Allelopathic mechanism of pyrogallol to Microcystis aeruginosa PCC7806 (Cyanobacteria): from views of gene expression and antioxidant system. Chemosphere 75, 924–928. https://doi.org/10.1016/j.chemosphere.2009.01.021.

Shi, Q., Tang, J., Wang, L., Liu, R., Giesy, J.P., 2021. Combined cytotoxicity of polystyrene nanoplastics and phthalate esters on human lung epithelial A549 cells and its mechanism. Ecotoxicol. Environ. Saf. 213, 112041 https://doi.org/10.1016/j.ecoenv.2021.112041.

Sobhani, Z., Lei, Y., Tang, Y., Wu, L., Zhang, X., Naidu, R., Megharaj, M., Fang, C., 2020. Microplastics generated when opening plastic packaging. Sci. Rep. 10, 4841. https://doi.org/10.1038/s41598-020-61146-4.

Song, Z.-Q., Wang, L., Wang, F.-P., Jiang, H.-C., Chen, J.-Q., Zhou, E.-M., Liang, F., Xiao, X., Li, W.-J., 2013. Abundance and diversity of archaeal accA gene in hot springs in Yunnan Province, China. Extremophiles 17, 871–879. https://doi.org/10.1007/s00792-013-0570-4.

Song, Y., Zhang, B., Si, M., Chen, Z., Geng, J., Liang, F., Xi, M., Liu, X., Wang, R., 2023. Roles of extracellular polymeric substances on Microcystis aeruginosa exposed to different sizes of polystyrene microplastics. Chemosphere 312, 137225. https://doi.org/10.1016/j.chemosphere.2022.137225.

Spencer, C.M., Cai, Y., Martin, R., Gaffney, S.H., Goulding, P.N., Magnolato, D., Lilley, T. H., Haslam, E., 1988. Polyphenol complexation—some thoughts and observations. Phytochemistry 27, 2397–2409. https://doi.org/10.1016/0031-9422(88)87004-3.

Sun, Y., Ren, X., Pan, J., Zhang, Z., Tsui, T.-H., Luo, L., Wang, Q., 2020. Effect of microplastics on greenhouse gas and ammonia emissions during aerobic composting. Sci. Total Environ. 737, 139856 https://doi.org/10.1016/j.scitotenv.2020.139856.

Sun, T., Wang, S., Ji, C., Li, F., Wu, H., 2022. Microplastics aggravate the bioaccumulation and toxicity of coexisting contaminants in aquatic organisms: a synergistic health hazard. J. Hazard. Mater. 424, 127533 https://doi.org/10.1016/j.jhazmat.2021.127533.

Sung, S.Y., Kim, S.H., Velusamy, V., Lee, Y.-M., Ha, B.-K., Kim, J.-B., Kang, S.-Y., Kim, H. G., Kim, D.S., 2013. Comparative gene expression analysis in a highly anthocyanin pigmented mutant of colorless chrysanthemum. Mol. Biol. Rep. 40, 5177–5189. https://doi.org/10.1007/s11033-013-2620-5.

Taghizadeh, S.-M., Berenjian, A., Chew, K.W., Show, P.L., Mohd Zaid, H.F., Ramezani, H., Ghasemi, Y., Raee, M.J., Ebrahiminezhad, A., 2020. Impact of magnetic immobilization on the cell physiology of green unicellular algae Chlorella vulgaris. Bioengineered 11, 141–153. https://doi.org/10.1080/21655979.2020.1718477.

Tillett, D., Dittmann, E., Erhard, M., Von Döhren, H., Börner, T., Neilan, B.A.J.C., biology, 2000. Structural organization of microcystin biosynthesis in Microcystis aeruginosa PCC7806: an integrated peptide–polyketide synthetase system. Chem. Biol. 7, 753–764. https://doi.org/10.1016/S1074-5521(00)00021-1.

Villegas, L., Cabrera, M., Moulatlet, G.M., Capparelli, M., 2022. The synergistic effect of microplastic and malathion exposure on fiddler crab Minuca ecuadoriensis microplastic bioaccumulation and survival. Mar. Pollut. Bull. 175, 113336 https://doi.org/10.1016/j.marpolbul.2022.113336.

Wang, J., Zhao, F., Chen, B., Li, Y., Na, P., Zhuo, J., 2013. Small water clusters stimulate microcystin biosynthesis in cyanobacterial Microcystis aeruginosa. J. Appl. Phycol. 25, 329–336. https://doi.org/10.1007/s10811-012-9867-4.

Wang, J., Liu, Q., Feng, J., Lv, J., Xie, S., 2016a. Photosynthesis inhibition of pyrogallol against the bloom-forming cyanobacterium Microcystis aeruginosa TY001. Pol. J. Environ. Stud. 25, 2601–2608. https://doi.org/10.15244/pjoes/63412.

Wang, J., Vine, C.E., Balasiny, B.K., Rizk, J., Bradley, C.L., Tinajero-Trejo, M., Poole, R. K., Bergaust, L.L., Bakken, L.R., Cole, J.A., 2016b. The roles of the hybrid cluster protein, Hcp and its reductase, Hcr, in high affinity nitric oxide reduction that protects anaerobic cultures of Escherichia coli against nitrosative stress. Mol. Microbiol. 100, 877–892. https://doi.org/10.1111/mmi.13356.

Wang, X., Miao, J., Pan, L., Li, Y., Lin, Y., Wu, J., 2019. Toxicity effects of p-choroaniline on the growth, photosynthesis, respiration capacity and antioxidant enzyme activities of a diatom, Phaeodactylum tricornutu. Ecotoxicol. Environ. Saf. 169, 654–661. https://doi.org/10.1016/j.ecoenv.2018.11.015.

Wang, S., Li, Q., Huang, S., Zhao, W., Zheng, Z., 2021a. Single and combined effects of microplastics and lead on the freshwater algae Microcystis aeruginosa. Ecotoxicol. Environ. Saf. 208, 111664 https://doi.org/10.1016/j.ecoenv.2020.111664.

Wang, W., Hou, Y., Pan, W., Vinay, N., Mo, F., Liao, Y., Wen, X., 2021b. Continuous application of conservation tillage affects in situ N2O emissions and nitrogen cycling gene abundances following nitrogen fertilization. Soil Biol. Biochem. 157, 108239 https://doi.org/10.1016/j.soilbio.2021.108239.

Wang, Q., Wang, J., Chen, H., Zhang, Y., 2023a. Toxicity effects of microplastics and nanoplastics with cadmium on the alga Microcystis aeruginosa. Environ. Sci. Pollut. Res. 30, 17360–17373. https://doi.org/10.1007/s11356-022-23278-0.

Wang, S., Zhang, X., Wang, C., Chen, N., 2023b. Multivariable integrated risk assessment for cyanobacterial blooms in eutrophic lakes and its spatiotemporal characteristics. Water Res. 228, 119367 https://doi.org/10.1016/j.watres.2022.119367.

Wang, X., Zhao, Y., Zhao, L., Wan, Q., Ma, L., Liang, J., Li, H., Dong, J., Zhang, M., 2023c. Effects of microplastics on the growth, photosynthetic efficiency and nutrient composition in freshwater algae Chlorella vulgaris Beij. Aquat. Toxicol. 261, 106615 https://doi.org/10.1016/j.aquatox.2023.106615.

Wei, C., Zhang, Y., Guo, J., Han, B., Yang, X., Yuan, J., 2010. Effects of silica nanoparticles on growth and photosynthetic pigment contents of Scenedesmus obliquus. J. Environ. Sci. 22, 155–160. https://doi.org/10.1016/S1001-0742(09)60087-5.

Wu, D., Wang, T., Wang, J., Jiang, L., Yin, Y., Guo, H., 2021. Size-dependent toxic effects of polystyrene microplastic exposure on Microcystis aeruginosa growth and microcystin production. Sci. Total Environ. 761, 143265 https://doi.org/10.1016/j.scitotenv.2020.143265.

Yang, M., Meng, F., Gu, W., Fu, L., Zhang, F., Li, F., Tao, Y., Zhang, Z., Wang, X., Yang, X., Li, J., Yu, J., 2021. Influence of polysaccharides from Polygonatum kingianum on short-chain fatty acid production and quorum sensing in Lactobacillus faecis. Front. Microbiol. 12 https://doi.org/10.3389/fmicb.2021.758870.

Yi, X., Chi, T., Li, Z., Wang, J., Yu, M., Wu, M., Zhou, H., 2019. Combined effect of polystyrene plastics and triphenyltin chloride on the green algae Chlorella pyrenoidosa. Environ. Sci. Pollut. Res. 26, 15011–15018. https://doi.org/10.1007/s11356-019-04865-0.

Yu, S., Xu, C., Tang, T., Zhang, Y., Effiong, K., Hu, J., Bi, Y., Xiao, X., 2023. Down-regulation of iron/zinc ion transport and toxin synthesis in Microcystis aeruginosa exposed to 5,4′-dihydroxyflavone. J. Hazard. Mater. 460, 132396 https://doi.org/10.1016/j.jhazmat.2023.132396.

Zhang, T.-T., Zheng, C.-Y., Hu, W., Xu, W.-W., Wang, H.-F., 2010. The allelopathy and allelopathic mechanism of phenolic acids on toxic Microcystis aeruginosa. J. Appl. Phycol. 22, 71–77. https://doi.org/10.1007/s10811-009-9429-6.

Zhang, W., Liu, X., Liu, L., Lu, H., Wang, L., Tang, J., 2022. Effects of microplastics on greenhouse gas emissions and microbial communities in sediment of freshwater systems. J. Hazard. Mater. 435, 129030 https://doi.org/10.1016/j.jhazmat.2022.129030.

Zhang, C., Lin, X., Gao, P., Zhao, X., Ma, C., Wang, L., Sun, H., Sun, L., Liu, C., 2023. Combined effects of microplastics and excess boron on Microcystis aeruginosa. Sci. Total Environ. 891, 164298 https://doi.org/10.1016/j.scitotenv.2023.164298.

Zhang, W., Wang, L., Liu, Q., Lyu, H., Tang, J., 2024. Adsorption of PCBs on microplastics mitigated greenhouse gas emission by changing C/N metabolism in freshwater sediment. J. Clean. Prod. 434, 139883 https://doi.org/10.1016/j.jclepro.2023.139883.

Zhen, M., Song, B., Liu, X., Chandankere, R., Tang, J., 2018. Biochar-mediated regulation of greenhouse gas emission and toxicity reduction in bioremediation of organophosphorus pesticide-contaminated soils. Chin. J. Chem. Eng. 26, 2592–2600. https://doi.org/10.1016/j.cjche.2018.01.028.

Zheng, X., Yuan, Y., Li, Y., Liu, X., Wang, X., Fan, Z., 2021a. Polystyrene nanoplastics affect growth and microcystin production of Microcystis aeruginosa. Environ. Sci. Pollut. Res. 28, 13394–13403. https://doi.org/10.1007/s11356-020-10388-w.

Zheng, X., Zhang, W., Yuan, Y., Li, Y., Liu, X., Wang, X., Fan, Z., 2021b. Growth inhibition, toxin production and oxidative stress caused by three microplastics in Microcystis aeruginosa. Ecotoxicol. Environ. Saf. 208, 111575 https://doi.org/10.1016/j.ecoenv.2020.111575.

Zhou, J., Gao, L., Lin, Y., Pan, B., Li, M., 2021. Micrometer scale polystyrene plastics of varying concentrations and particle sizes inhibit growth and upregulate microcystin-related gene expression in Microcystis aeruginosa. J. Hazard. Mater. 420, 126591 https://doi.org/10.1016/j.jhazmat.2021.126591.

Zhu, Z.-L., Wang, S.-C., Zhao, F.-F., Wang, S.-G., Liu, F.-F., Liu, G.-Z., 2019. Joint toxicity of microplastics with triclosan to marine microalgae Skeletonema costatum. Environ. Pollut. 246, 509–517. https://doi.org/10.1016/j.envpol.2018.12.044.

Zhu, X., Dao, G., Tao, Y., Zhan, X., Hu, H., 2021. A review on control of harmful algal blooms by plant-derived allelochemicals. J. Hazard. Mater. 401, 123403 https://doi.org/10.1016/j.jhazmat.2020.123403.

Zilliges, Y., Kehr, J.-C., Meissner, S., Ishida, K., Mikkat, S., Hagemann, M., Kaplan, A., Börner, T., Dittmann, E., 2011. The cyanobacterial hepatotoxin microcystin binds to proteins and increases the fitness of microcystis under oxidative stress conditions. PLoS One 6, e17615. https://doi.org/10.1371/journal.pone.0017615.